Monte-Carlo Simulation of Branching Distribution in Ni-Diimine Catalyzed Polyethylene

Leonardo C. Simon, Joao B. P. Soares, and Roberto F. de Souza
Institute for Polymer Research, Dept. of Chemical Engineering, University of Waterloo, Waterloo, Ontario, Canada, N2L 3G1

Monte-Carlo simulation was used to study the short-chain branch formation of polyethylene made with a Ni-diimine catalyst. Branches are formed through the chain-walking mechanism without any comonomer addition. The model describes the type of branch, that is, methyl, ethyl, propyl, butyl, pentyl, hexyl, heptyl, octly, nonyl, and decyl (or longer branches) and the distribution of these branches in the backbone, showing information that cannot be accessed by ^{13}C NMR. The branching structure of these polymers seems to be determined by two major kinetic steps described by the following model parameters: a beta transfer parameter describing the ratio of monomer insertion to beta hydrogen transfer and an isomerization barrier parameter controlling the ratio among different types of branches. The model showed that methyl branches are favored on the other branches in the chain-walking mechanism. The branch distribution obtained with the model developed herein agrees well with ^{13}C NMR experimental results.

Introduction

The search of more efficient catalytic systems for production of tailor-made polyolefins has been a point of great interest lately (Morse, 1998). Polyethylene with controlled molecular-weight distribution and different degrees of short-chain branching (SCB) can be produced with single-site-type metallocene catalytic systems (Soares and Hamielec, 1996; Hamielec and Soares, 1995; Olabisi et al., 1997). SCB changes the morphology of the polymer crystals and affects several physical and rheological properties (Minick et al., 1995). The SCB in polyethylene produced by metallocene and conventional Ziegler-Natta catalysts is formed by copolymerization of ethylene and α-olefin.

Brookhart and coworkers (Johnson et al., 1995) have shown that the combination of nickel-diimine complexes and methylaluminoxane (MAO) is able to produce polyethylene with different degrees of methyl and longer branches without the addition of comonomers. The branches are formed by a mechanism called ‘‘chain walking.’’ The diimine ligands have a strong influence in the microstructure of products formed in the polymerization (Johnson et al., 1995; Schleis et al., 1998).

De Souza (1997) and Simon (1999) have shown that chlorine-free aluminum compounds other than MAO can activate the Ni-diimine complex and that the degree of branching can be easily controlled by polymerization temperature. It was shown (Galland et al., 1999; Jurkiewicz et al., 1999) by ^{13}C NMR studies that these polyethylenes have different types of short branches, from methyl to hexyl and longer branches.

In this work we developed a Monte-Carlo model to simulate the chain-walking mechanism. The model can be used to predict the branching structure and molecular weight of polymers made with these catalysts. When compared with experimentally measured structural information, this model can be useful tool to investigate the mechanism of chain walking.

Chain-walking mechanism

Nickel complexes have been industrially used in olefin dimerization (Dimersol, Institute Francais du Petrole) (Chauvin et al., 1974) and oligomerization (SHOP, Shell) (Keim et al., 1981). Recently the University of North Carolina and E.I. du Pont de Nemours and Co., Inc., have developed an olefin polymerization process (Versipol) that uses Ni-diimine complexes as catalyst precursor (UNC/duPont, 1996). These nickel catalyst systems can produce polyethylene with controlled degrees of SCB. This feature is due to

---

Correspondence concerning this article should be addressed to J. B. P. Soares.
Present address of R. F. de Souza: Instituto de Química, Universidade Federal do Rio Grande do Sul, Porto Alegre, Brasil.

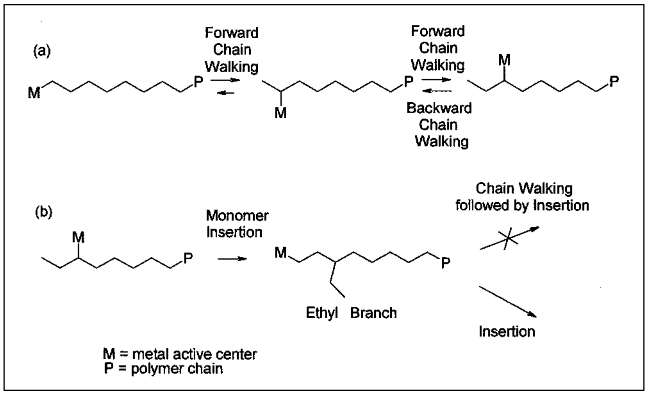

Figure 1. Chain-walking mechanism.

(a) Chain walking can occur in both directions: forward chain walking—from the terminal carbon toward the center; backward chain walking—from the center of the chain toward the chain end; and (b) chain walking is likely not to take place just after branch formation.

the chain-walking mechanism that takes place during polymerization with these catalysts.

In the chain-walking mechanism (Brookhart et al., 1996; McLain et al., 1997; Schleis et al. 1998; Simon et al., 1999) the active center moves along the growing polymer chain. The process starts when a β-hydride elimination followed by reinsertion, that is, β-hydride shift or β-hydride transfer, occurs instead of a monomer addition. In this process the active site moves from the terminal carbon in the polymer chain to the next carbon in the backbone. This chain-walking step can be repeated several times before monomer is added to the chain or the chain is terminated. A monomer insertion after a chain-walking step produces a branch. Figure 1 illustrates a simplified scheme of this mechanism.

Chain walking is believed to occur in both directions, that is, from the terminal carbon toward the center of the backbone, and from any internal carbon backward to the terminal carbon. The active center is unlikely to migrate to the two carbons next to a tertiary branch point. Consequently, this assumption precludes the formation of branches in consecutive carbons or separated by one carbon atom. For the same reason, chain walking does not take place immediately after branch formation. It is necessary that another monomer molecule be inserted after branch formation for chain walking to occur. ^{13}C NMR data have shown that two or more carbons separate branches. There is no evidence of branches on branches, branches linked to consecutive carbons in the backbone, or branches separated by only one carbon (Jurkiewicz et al., 1999; Galland et al., 1999). A different behavior was reported for Pd-diimine catalyzed polyethylene (Guan et al., 1999), where branches on branches were found.

A β-hydrogen elimination reaction starts the chain-walking mechanism and occurs whenever the active site walks through the backbone. The chain transfer is suppressed by the diimine ligand bulkiness. Indeed during the chain-walking mechanism an isomerization process takes places—that is, through the elementary reaction steps, β-hydrogen elimination/reinsertion—the active center changes its position in the backbone without the occurrence of chain transfer.

Model Description

A Monte-Carlo model was developed to simulate the branching structure and the molecular-weight distribution of polymer made with catalyst that undergoes chain walking. A long period ($> 2 \times 10^{18}$) random number generator of L'Ecuyer with Bays-Durham shuffle is used to generate model probabilities (Press et al., 1992).

The model input consist of five parameters: (a) r_n (number average of insertion events); (b) P_β (probability of β-transfer); (c) P_i (probability of isomerization barrier); (d) P_f (probability of forward chain walking); and (e) P_m (probability of methyl favoring). These parameters were necessary to better describe our experimental findings. The probability of chain termination is obtained from r_n, by noticing that

$$r_n = \frac{1}{P_\beta P_t}, \tag{1}$$

and therefore

$$P_t = \frac{1}{P_\beta r_n}. \tag{2}$$

The sequence of model events is illustrated in Figure 2. A more detailed flow chart is given in Figure 3.

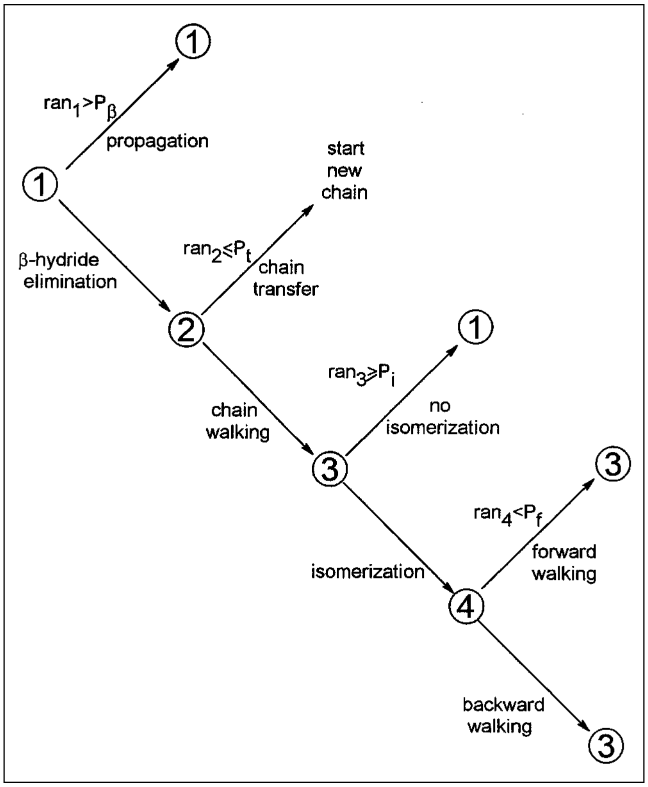

Figure 2. Sequence of events during Monte-Carlo simulation of polymerization and chain walking.

P_β: probability of β-transfer; P_t: probability of chain termination; P_i: probability of isomerization barrier; P_f: probability of forward chain walking.

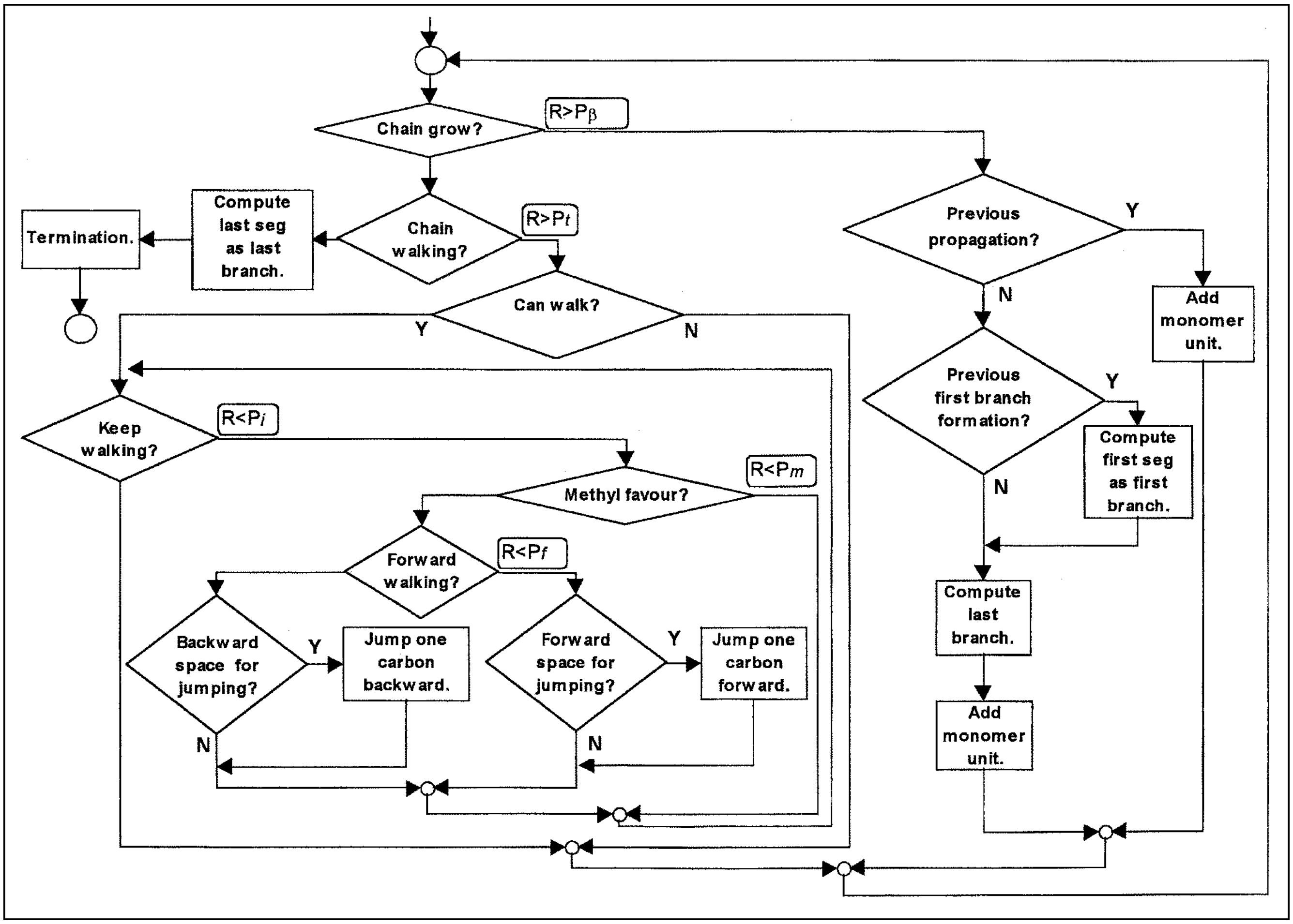

Figure 3. Computer program for Monte-Carlo simulation.

R: random number; P_β: probability of β-transfer P_t: probability of chain termination; P_i: probability of isomerization barrier; P_m: probability of methyl favoring; P_f: probability of foward chain walking.

A random number is generated to decide between two possible outcomes of an elementary step. The numbers shown in Figure 2 indicate random number generations. If $ran_1, > P_\beta$, a monomer insertion takes place. One monomer unit is added to the chain backbone and the random number generator is called again. If $ran_1, \leq P_\beta$, a β-hydride elimination step takes place and the random number generation is called to decide between the two next steps. If $ran_2 \leq P_t$, the chain is terminated, all structural information recorded, and a new chain is started until the total number of chains is generated. If $ran_2 > P_t$, the chain-walking computational procedure starts. First, the program tests if chain walking is feasible according to the current experimental knowledge about chain structure made with this mechanism. Therefore, the minimum number of carbons between branches is fixed at 2 and no branches on branches are allowed (that is, the active site cannot "walk" past the last branch point). If chain walking is not feasible, the program returns to the insertion decision step (Figure 2, step 1). If chain walking is feasible, a third random number is generated, ran_3, to test for the probability of isomerization barrier. This probability determines the extension of chain walking, by deciding how many times the active center will "walk" on the polymer backbone before a monomer insertion or chain termination step takes place. If $ran_3 \geq P_i$, isomerization does not take place and the program returns to the monomer insertion decision step. If $ran_3 < P_i$, either forward or backward chain walking will take place, according to the value of ran_4. If $ran_4 < P_f$, the active site will move one carbon atom away from the terminal carbon, which is forward chain walking (provided there is space). Movement in the opposite direction, backward chain walking, will take place if $ran_4 \geq P_f$. The probability of forward chain walking affects the direction only if the active site is located in one of the five first carbons of the chain. Beyond the fifth carbon from the chain end, P_f is considered to be 0.5, that is, there is no preference in the chain-walking direction anymore. After one step of chain walking takes place, the program returns to the probability of isomerization barrier decision step (Figure 2, step 3) and the process is repeated until $ran_3 \geq P_i$.

The probability of methyl favoring, P_m, is used to increase the number of methyl branches upon the other types of branches. If there is a suitable condition for methyl-branch formation and $ran \leq P_m$, the chain-walking mechanism is avoided and the methyl branch is formed. When a large value is assigned to this probability, the likelihood of methyl branch formation is increased. This probability was included in the

Table 1. Short-Chain Branch Distribution Generated with Monte-Carlo Simulation

	Simulation Parameters				SCB/1,000 C in the Backbone										
Entry	P_β	P_i	P_f	P_m	Me	Et	Pr	Bu	Pt	Hx	Hp	Oc	No	De+	Total
1	0.1	0.1	0.5	0.0001	2.49	0.14	0.01	0.00	0.00	0.00	0.00	0.00	0.00	0.21	2.86
2	0.9	0.1	0.5	0.0001	83.76	18.57	5.15	1.29	0.57	0.26	0.22	0.14	0.15	0.86	110.99
3	0.25	0.5	0.5	0.0001	26.34	7.67	2.39	0.71	0.23	0.07	0.03	0.02	0.01	0.21	37.68
4	0.25	0.95	0.5	0.0001	31.02	19.01	13.26	8.60	6.04	3.98	2.79	1.85	1.30	2.83	90.68
5	0.25	0.95	0.1	0.0001	11.57	1.20	0.13	0.02	0.00	0.00	0.00	0.00	0.00	0.24	13.17
6	0.25	0.95	0.7	0.0001	26.39	19.22	16.95	13.95	14.99	11.68	7.89	4.80	3.29	6.34	125.50
7	0.25	0.95	0.7	0.5	40.71	15.79	14.12	12.12	13.07	10.21	6.91	4.19	2.88	5.54	125.53
8	0.25	0.95	0.7	0.9	76.94	6.79	6.34	6.20	6.75	5.34	3.62	2.19	1.51	2.92	118.60
9	0.86	0.9	0.99	0.1	137.75	70.42	68.00	10.74	12.02	1.95	0.88	0.15	0.06	0.02	302.00
10*	0.9	0.99	0.5	0.0001	85.09	37.73	22.78	8.50	5.32	1.86	1.17	0.35	0.21	0.12	163.12
11	0.257	0.94	0.7	0.814	66.69	10.25	9.22	8.24	8.66	6.65	4.42	2.59	1.75	3.13	121.62
12	0.226	0.94	0.7	0.797	55.56	9.36	8.42	7.63	8.19	6.47	4.33	2.61	1.77	3.30	107.64

Note: *All simulations were run with $r_n = 5{,}000$.
Branches per 1,000 C in the polymer chain.

model as an additional parameter to help explain the dominance of methyl over other branch types. The use of P_m is explained in Figure 3, but not shown in Figure 2. The predominance of methyl branches seems to be intrinsic to the chain-walking mechanism. Without the use of P_m—methyl favoring parameter—the model cannot properly fit the ratio between methyl and ethyl branches, but the ratio among branches longer than two carbons, such as ethyl to propyl, propyl to butyl, butyl to pentyl, and so on, is well represented even if P_m is not used. The parameter P_m seems to be related to the mechanism involved in the competition between β-hydride elimination/reinsertion (isomerization) and ethylene insertion when the active site is bound to the next-to-the-last carbon of the growing polymer chain.

The probability of forward chain walking, P_f, was used to investigate the effect of the direction of the active site migration during chain walking. It is reasonable to assume that the chain end can affect the direction of chain walking if the active site is located near the chain end. However, it is also reasonable to assume that chain end effects will be negligible if the active site is far removed from the end of the backbone. We arbitrarily decided to set a ‘‘cutoff’’ point at five carbons away from the chain end. Consequently, if the active site is placed on the sixth or farther removed carbon from the chain end, P_f is set of 0.5. This is evidently a model simplification, since the effect of the chain end is likely a gradual one (that is, P_f is most likely to vary continuously from the carbon to carbon), but a more precise determination of this dependency is beyond the scope of this study. Nonetheless, this simple approach permitted a better fit of the experimental results. In the light of this observation, we believe that when the active site is close to the chain end there is a small preference of chain walking occurring in the forward direction, that is, away from the chain end. This result can be observed by comparing entries 4–6 in Table 1.

Table 2. Nomenclature for Type and Relative Position of Short-Chain Branches Formed by the Chain-Walking Mechanism

Relative Position to Next Branch	Branch Type
$\delta+$	Me—methyl
1,4	Et—ethyl
1,5	Pr—propyl
1,6	Bu—butyl
	Pt—pentyl
	Hx—hexyl
	Hp—heptyl
	Oc—octyl
	No—nonyl
	De+—decyl or longer branches

Moreover, a critical observation could be made to the restriction imposed in the model on the migration of the active site next to a branch. The assumption that the active site does not migrate toward the two carbons next to a branch comes from the experimental observations. No adjacent branches have been detected from ^{13}C NMR studies. This experimental finding indicates that (1) active sites do not migrate to the two carbons adjacent to a branch, or (2) if migration occurs, no ethylene insertion takes place at these positions, maybe for steric reasons. Although this mechanism's subtlety is not known at the moment, from a modeling point of view this can be easily introduced by restricting active site migration to the two carbons next to a branch. This is the option adopted in the model proposed herein.

The model keeps track of up to 10 branch sizes: methyl, ethyl, propyl, butyl, pentyl, hexyl, heptyl, octyl, nonyl, and decyl+. Branches with 10 carbon atoms or more are counted as decyl+branches. The program also registers the relative position of the neighbor branch spaced 2 carbons (1,4 relative position), 3 carbons (1,5 relative position), 4 carbons (1,6 relative position) away, or no near neighbor at least up to the next 5 adjacent carbons ($\delta+$). The nomenclature used to indicate the relative position of the right and left neighbors and the branch type is described in Table 2 (Galland et al., 1999).

The computer program to perform the Monte-Carlo simulation was written in ANSI/ISO Draft Standard C++ computer language. The simulations were run using a Pentium II processor. A copy of the executable code can be obtained free of charge from the authors.

Experimental Methods

The polyethylene samples shown in Table 3 were synthesized using Ni-diimine catalyst with triisobutyl aluminum

Table 3. Short-Chain Branch Distribution by ^{13}C NMR Analysis of Polyethylene Produced with Nickel-Diimine Catalytic System (Simon et al., 1999) and by Monte-Carlo Simulation of Chain-Walking Mechanism

Branch Type	Sample 1			Sample 2		
	^{13}C NMR (SCB/1,000 C)	Ratio*	Simulation** (SCB/1,000 C)	^{13}C NMR (SCB/1,000 C)	Ratio*	Simulation† (SCB/1,000 C)
Methyl	55.4	5.5	55.56	66.6	4.8	66.69
Ethyl	10.1	1.0	9.36	13.8	3.7	10.25
Propyl	10.6	1.0	8.42	3.7	0.3	9.22
Butyl	11.1	3.2	7.63	11.4	3.3	8.24
Pentyl	3.5	0.2	8.19	3.5	0.2	8.66
Hexyl+††	16.8		18.48	22.5		18.54
Total	107.5		107.64	121.5		121.62

*Ratio between the number of branches with n carbons and the number of branches with $n+1$ carbons, related to ^{13}C NMR results.
**Values corresponding to entry 12 in Table 1.
†Values corresponding to entry 11 in Table 1.
††Hexyl+: hexyl and longer branches.

(Sample 1) and trimethyl aluminum (Sample 2) as cocatalyst, through homogeneous polymerization using chlorobenzene as solvent, at 1.080 atm of ethylene pressure, a temperature of 30°C, and 2-h polymerization time. More detailed information was published elsewhere (Simon et al., 1999). ^{13}C NMR quantitative analysis was performed using a Varian Inova 300-MHz spectrometer operating at 75 MHz, at 80°C, with a 75° flip angle, an acquisition time of 1.5 s, and a delay of 4.0 s (Galland et al., 1999).

Results and Discussions

The SCB distribution obtained with our simulation model is in good agreement with that obtained by ^{13}C NMR experimental results, as shown in Table 3. Model parameters for these simulations are shown in Table 1, entries 11 and 12. The model gives information about branches longer than 7 carbons that is not accessible by NMR spectroscopy.

The parameters for the ‘‘best’’ simulation results shown in Table 3 were found by trial-and-error during the parameter sensitivity analysis shown in Table 1. It is likely that an even better fit could be obtained using a more sophisticated optimization routine, but the objective of this article is only to study the leading parameters affecting branching structure. The good description of the branching structure given by the model is a strong indication that the model steps are likely to be correct. The effect of each parameter on the branching structure is discussed next.

An increase in P_β increases the total number of branches in the polymer (entries 1 and 2, Table 1) as expected. Nevertheless, for $P_i = 0.1$, the ratio between the number of branches with n carbons, and the number of branches with $n+1$ carbons does not agree with the ratios observed experimentally (entries 1 and 2, Table 4). Simulated branching frequencies decrease steadily from methyl to decyl+, while experimental results show that methyl branches dominate, although the other branches are present at about the same branching frequency. To change this behavior we need to change P_i. Increasing P_i leads to a more uniform distribution (entries 3 and 4, Tables 1 and 4). It is interesting to note that an increment in this parameter also increases the total branch content.

The P_f parameter was studied with the objective of identifying some preference in the direction of the active center migration. Analyzing entries 4, 5, and 6 (Tables 1 and 4), one concludes that forward chain walking increases the total branch content and produces a more uniform branch distribution. On the other hand, backward chain walking decreases the total branch content and shorter branches are formed.

The P_m parameter has a minor effect over the total branch content. Its main function is to modulate the ratio between the amount of methyl and ethyl branches. When P_m increases, the amount of the methyl branch increases in detriment of other branch types, as can be seen from entries 6, 7 and 8 in Tables 1 and 4.

Table 4. Ratio* between Branch with n Carbons and $n+1$ Carbons, from the Monte-Carlo Simulation Model of Chain-Walking Mechanism

Entry	Simulation Parameters				Ratio Between Branch With n Carbons and $n+1$ Carbons								
	P_β	P_i	P_f	P_m	Me/Et	Et/Pr	Pr/Bu	Bu/Pt	Pt/Hx	Hx/Hp	Hp/Oc	Oc/No	No/De+
1	0.1	0.1	0.5	0.0001	19	18	6	4	1	1	0	2	0
2	0.9	0.1	0.5	0.0001	4	4	4	2	2	1	2	1	0
3	0.25	0.5	0.5	0.0001	3	3	3	3	3	3	2	2	0
4	0.25	0.95	0.5	0.0001	2	1	2	1	2	1	2	1	0
5	0.25	0.95	0.1	0.0001	10	10	8	4	1	1	1	1	0
6	0.25	0.95	0.7	0.0001	1	1	1	1	1	1	2	1	1
7	0.25	0.95	0.7	0.5	3	1	1	1	1	1	2	1	1
8	0.25	0.95	0.7	0.9	11	1	1	1	1	1	2	1	1
9	0.9	0.99	0.5	0.0001	2	2	3	2	3	2	3	2	2

*These ratios correspond to entries 1–9 in Table 1.

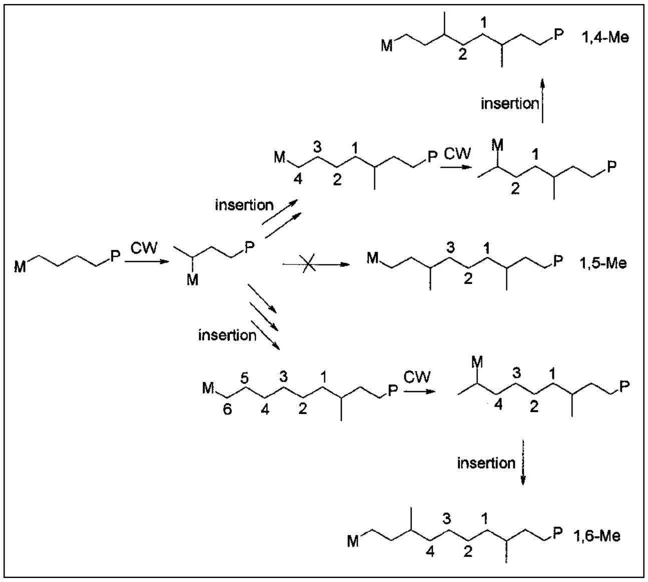

Figure 4. In the chain-walking simulation model, two methyl branches (or any other branch with an odd number of carbon atoms) cannot be separated by 3 C atoms (or any odd number of carbon atoms).

CW: chain walking.

Table 5. Relative Position Distribution of Branches by Monte-Carlo Simulation of Chain-Walking Mechanism

Branch to Neighbors Positions	SCB/1,000 C Backbone									
	Me	Et	Pr	Bu	Pt	Hx	Hp	Oc	No	De+
$\delta+-\delta+$	13.9	2.7	2.0	2.2	2.3	2.3	1.3	1.0	0.6	1.2
$1{,}4-\delta+$	15.3	1.2	2.3	1.0	2.1	1.0	1.1	0.4	0.4	0.6
$1{,}5-\delta+$	2.7	2.7	0.4	2.2	0.4	1.5	0.2	0.6	0.1	0.0
$1{,}6-\delta+$	9.8	0.8	1.6	0.6	1.5	0.7	0.8	0.3	0.3	0.4
1,4–1,4	4.0	0.0	0.6	0.0	0.5	0.0	0.2	0.0	0.1	0.1
1,4–1,5	1.8	0.9	0.3	0.8	0.2	0.5	0.1	0.2	0.0	0.2
1,4–1,6	5.3	0.0	0.8	0.0	0.7	0.0	0.3	0.0	0.1	0.0
1,5–1,5	0.0	0.4	0.0	0.3	0.0	0.2	0.0	0.1	0.0	0.5
1,5–1,6	1.1	0.6	0.2	0.5	0.2	0.3	0.1	0.1	0.0	0.1
1,6–1,6	1.7	0.0	0.3	0.0	0.2	0.0	0.1	0.0	0.1	0.0

Note: This SCB distribution corresponds to entry 12 in Table 1.

It is important to establish the base on which the branches are being accounted when dealing with macromolecules having high branching degree and different types of branches. Entries 9 and 10 in Table 1 show how different the results are when a distinction is made between the number of branches per 1,000 C in the molecule instead of 1,000 C in the backbone. Entry 9, where the probability parameters are set to produce a high branch content, shows a polymer with 302 branches per 1,000 C of the backbone, which is near the limit of 333 branches per 1,000 C of the backbone as established in the model.

Branch position

The results obtained with the model also elucidate the different neighbors that each type of branch can have. According to the proposed model, the branches with an odd number of carbons cannot have both neighbors at 1,5 relative positions, that is, separated by 3 carbons, 1,5-Me-1,5, for instance. This feature of the chain-walking mechanism is illustrated in Figure 4. The methyl branch can only have a neighbor in the relative position 1,5 if this neighbor has an even number of carbon atoms, such as an ethyl branch.

Similarly, branches with an even number of carbons cannot have both neighbors in 1,4 and/or 1,6 relative positions. Table 5 clearly describes such result.

SCB and molecular weight

The molecular-weight distribution of these polymers obtained by Monte-Carlo simulation follows Flory's distribution (Flory, 1953). According to the proposed model, the probability of chain termination, P_t, has no effect on the chain-walking mechanism, and therefore does not change branching frequencies.

All polymer molecules produced in each simulation run have approximately the same number of SCB per 1,000 C atoms of the backbone, as shown in Figure 5. The small fluctuations observed are due to statistical variances in Monte-Carlo simulations and would be eliminated if a larger number of chains were generated.

This result also confirms the assumption that the chain-walking mechanism is not affected by the size of the growing polymer chain.

Conclusions

The short-chain branching distribution produced by the chain-walking mechanism for ethylene polymerization with Ni-diimine catalyst was studied with Monte-Carlo simulation. The model has shown that different kinds of SCB can be formed, such as methyl, ethyl, propyl, butyl, pentyl, hexyl, heptyl, octyl, nonyl, and decyl+ branches. Some branch con-

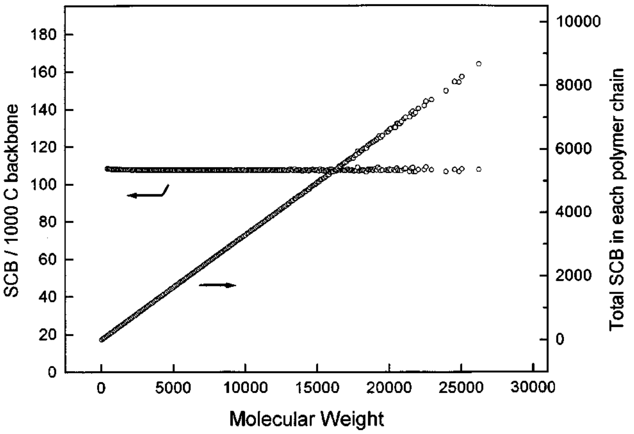

Figure 5. SCB distribution as a function of molecular weight obtained with Monte-Carlo model.

Results corresponding to parameters in entry 12, Table 1. $r_n = 5{,}000$ and number of chains = 1,000,000.

figurations along the backbone cannot be attained. Branches with an odd number of carbons are not found separated from both neighbor branches by an odd number of carbon atoms, that is, 1,5-Me-1,5. A similar behavior was found for branches with an even number of carbon atoms separated by an even number of carbon atoms.

The SCB distribution obtained by the chain-walking mechanism can be described with the use of five parameters: (a) r_n (number average of insertion events); (b) P_β (probability of β-transfer); (c) P_i (probability of isomerization barrier); (d) P_f (probability of forward chain walking); and (e) P_m (probability of methyl favoring). The need for this last parameter to improve the fit of the experimental ^{13}C NMR results suggests that after the active center has moved from the terminal carbon of the backbone to the next one there is an increased probability of a monomer insertion step to occur than another chain-walking step.

The average molecular weight does not change the SCB distribution. The molecular weight follows the Flory distribution. The SCB are equally distributed over all molecules of the same simulation run, independently of the molecular weight of each polymer molecule.

The short-chain branching distribution for methyl, ethyl, propyl, butyl, and pentyl can be obtained by ^{13}C NMR spectroscopy. The proposed model parameters are optimized to fit these results. However, and perhaps more importantly, information on branches longer than six carbons, such as heptyl, octyl, and nonyl, which cannot be measured experimentally, can be predicted as well with this model. Additionally, the branching distribution present in Table 5 cannot be measured experimentally. These results show that the number of carbons in each branch precludes some relative positions for this branch in the backbone. The uniform branch distribution along the molecular-weight distribution should also be recognized as an important prediction. This result is, in fact, of great value to the polymer reaction engineering field, because it can be used to identify concomitant mechanisms acting during polymerization.

Acknowledgments

Leonardo Coelho Simon thanks CAPES for the fellowship.

Literature Cited

Brookhart, M., L. K. Johnson, C. M. Killian, S. Mecking, and D. J. Tempel, ‘‘Palladium(II)- and Nickel(II)-Catalyzed Olefin Polymerization,’’ *Poly. Preprint— Amer. Chem. Soc. Div. Polyn. Chem.*, **37**, 254 (1996).

Chauvin, Y., J. F. Gaillard, D. V. Quandg, and J. S. Andrews. ‘‘The IFP Dimersol Process for the Dimerisation of C_3 and C_4 Olefinic Cuts,’’ *Chem. Ind.*, 375 (1974).

De Souza, R. F., R. S. Mauler, L. C. Simon, F. F. Nunes, D. V. S. Vescia, and A. Cavagnolli, ‘‘[η^3-Methallyl-Nickel-Dad]PF_6 Complex: New Catalyst Precursor for Ethylene Polymerization,’’ *Macromol. Rapid Commun.*, **18**, 795 (1997).

Flory, P. J., *Principles of Polymer Chemistry*, Cornell Univ. Press, Ithaca, NY (1953).

Galland, G. B., R. F. de Souza, R. S. Mauler, and F. F. Nunes, ‘‘^{13}C Determination of the Composition of Linear Low-Density Polyethylene Obtained with ‘‘[η^3-Methallyl-Nickel-Dad]PF_6 Complex,’’ *Macromol.*, **32**, 1620 (1999).

Guan, Z., P. M. Cotts, E. F. McCord, and S. J. McLain, ‘‘Chain Walking: A New Strategy to Control Polymer Topology,’’ *Science*, **283**, 2059 (1999).

Jurkiewicz, A., N. W. Eilerts, and E. T. Hsieh, ‘‘^{13}C NMR Characterization of Short Chain Branches of Nickel Catalyzed Polyethylene,’’ *Macromol.*, **32**, 5471 (1999).

Hamielec, A. E., and J. B. P. Soares, ‘‘Polymerization Reaction Engineering—Metallocene Catalysis,’’ *Prog. Poly. Sci.*, **21**, 651 (1996).

Johnson, L. K., C. M. Killian, and M. Brookhart, ‘‘New Pd(II)- and Ni(II)-Based Catalysts for Polymerization of Ethylene and α-Olefins,’’ *J. Amer. Chem. Soc.*, **117**, 6414 (1995).

Keim, W., R. Appel, A. Storeck, C. Krueger, and R. Goddard, ‘‘Novel Nickel- and Palladium-Compexes with Aminobis(imino)phosphorane Ligands for the Polymerization of Ethylene,’’ *Angew. Chem. Int. Ed. Engl.*, **20**, 116 (1981).

McLain, S. J., E. F. McCord, L. K. Johnson, S. D. Ittel, L. T. J. Nelson, S. D. Arthur, M. J. Halfhill, M. F. Teasley, D. J. Tempel, C. Killian, and M. S. Brookhart, ‘‘^{13}C and 2D NMR of Novel Ethylene and Olefin Polymers Made with New Late Metal Catalysts,’’ *Poly. Preprint— Amer. Chem. Soc. Div. Poly. Chem.*, **38**, 772 (1997).

Minick, J., A. Moet, A. Hiltner, E. Baer, and S. P. Chum, ‘‘Crystallization of Very Low Density Copolymers of Ethylene with α-Olefins,’’ *J. Appl. Poly. Sci.*, **58**, 1371 (1995).

Morse, P. M., ‘‘New Catalysts Renew Polyolefins,’’ *Chem. Eng. News*, **27**, 11 (1998).

Olabisi, O., M. Atiqullah, and W. Kaminsky, ‘‘Group 4 Metallocenes: Supported and Unsupported Catalysts for Olefin Polymerization,’’ *J. Macromol. Sci.— Rev. Macromol. Chem. Phys.*, **C37**, 519 (1997).

Press, W. H., S. A. Teukolsky, W. T. Vetterling, and B. P. Flannery, *Numerical Recipes in C. The Art of Scientific Computing*, Cambridge Univ. Press, New York (1992).

Schleis, T., T. P. Spaniol, J. Okuda, J. Heinemann, and R. Mulhaupt, ‘‘Ethylene Polymerization Catalysts Based on Nickel(II) 1,4 Diazadiene Complexes: The Influence of the 1,4-Diazadiene Backbone Substitutes on Structure and Reactivity,’’ *J. Organomet. Chem.*, **569**, 159 (1998).

Simon, L. C., R. F. de Souza, and R. S. Mauler, ‘‘Effect of Alkylaluminum Cocatalyst on Ethylene Polymerization by Nickel-Diimine Complex,’’ *J. Poly. Sci. A: Polym. Chem.*, **37**, 4656 (1999).

Soares, J. B. P., and A. E. Hamielec, ‘‘Metallocene/Aluminoxane Catalysts for Olefin Polymerization. A Review,’’ *Poly. React. Eng.*, **3**, 131 (1995).

University of North Carolina and E. I. du Pont de Nemours and Co., Inc., Pat. Appl. WO 96-23,010 (1996).

Manuscript received Oct. 4, 1999, and revision received Dec. 21, 1999.